

Available online at www.sciencedirect.com

ScienceDirect

journal homepage: www.elsevier.com/locate/AJPS

Original Research Paper

Dissolvable polymeric microneedles loaded with aspirin for antiplatelet aggregation



Baorui Wang^{a,b}, Suohui Zhang^{a,c}, Guozhong Yang^c, Zequan Zhou^a, Mengzhen Xing^a, Han Liu^a, Aguo Cheng^a, Yunhua Gao^{a,b,c,*}

^aKey Laboratory of Photochemical Conversion and Optoelectronic Materials, Technical Institute of Physics and Chemistry of Chinese Academy of Sciences, Beijing 100190, China

^bSchool of Future Technology, University of Chinese Academy of Sciences, Beijing 101408, China

^cBeijing CAS Microneedle Technology Ltd, Beijing 102609, China

ARTICLE INFO

Article history:

Received 18 May 2022

Revised 20 October 2022

Accepted 11 January 2023

Available online 17 January 2023

Keywords:

Aspirin

Transdermal drug delivery

Polymeric microneedles

Hydrolysis

Antiplatelet aggregation

ABSTRACT

To reduce mucosal damage in the gastrointestinal tract caused by aspirin, we developed a dissolvable polymeric microneedle (MN) patch loaded with aspirin. Biodegradable polymers provide mechanical strength to the MNs. The MN tips punctured the cuticle of the skin and dissolved when in contact with the subcutaneous tissue. The aspirin in the MN patch is delivered continuously through an array of micropores created by the punctures, providing a stable plasma concentration of aspirin. The factors affecting the stability of aspirin during MNs fabrication were comprehensively analyzed, and the hydrolysis rate of aspirin in the MNs was less than 2%. Compared to oral administration, MN administration not only had a smoother plasma concentration curve but also resulted in a lower effective dose of antiplatelet aggregation. Aspirin-loaded MNs were mildly irritating to the skin, causing only slight erythema on the skin and recovery within 24 h. In summary, aspirin-loaded MNs provide a new method to reduce gastrointestinal adverse effects in patients requiring aspirin regularly.

© 2023 Published by Elsevier B.V. on behalf of Shenyang Pharmaceutical University.

This is an open access article under the CC BY-NC-ND license

(<http://creativecommons.org/licenses/by-nc-nd/4.0/>)

1. Introduction

Aspirin has significantly reduced morbidity and mortality related to coronary artery disease and is considered as the most cost-effective drug for secondary prevention of coronary artery disease [1]. Aspirin is a first-line antiplatelet

aggregation drug widely recognized for all types of platelet-dependent thrombotic vessel occlusion [2]. Aspirin is a non-selective cyclooxygenase (COX-1 and COX-2) inhibitor that inhibits the production of thromboxane A₂ (TXA₂) by inhibiting the activity of COX-1 [3,4]. The oral bioavailability of aspirin is approximately 40%–50% [5]. Low bioavailability has been reported for enteric tablets and sustained-release

* Corresponding author.

E-mail address: yhgao@mail.ipc.ac.cn (Y. Gao).

Peer review under responsibility of Shenyang Pharmaceutical University.

formulations of aspirin [6]. Oral aspirin requires large and frequent doses. Aspirin undergoes extensive hydrolysis to salicylic acid in the gastrointestinal tract and liver, with no antiplatelet aggregation activity. The half-life of aspirin in the plasma is approximately 15–20 min [7]. Although aspirin is rapidly cleared from the plasma, the antiplatelet aggregation effect persists owing to the irreversible inactivation for platelet COX-1 by aspirin [8,9]. The average lifespan of human platelets is approximately 10 d [10]. Therefore, continuous dosing is necessary to achieve long-term antiplatelet aggregation.

Long-term oral aspirin administration is associated with an increased risk of mucosal damage in the gastrointestinal tract [11]. These gastrointestinal adverse effects may be partly due to the local action of aspirin. One hypothetical mechanism is the direct stimulation of the gastrointestinal mucosa by aspirin, which leads to mucosal cell necrosis and capillary hemorrhage [12,13]. Another possible mechanism is the inhibition of COX-1 by aspirin. COX-1 catalyzes the synthesis of gastric prostaglandins. Gastric prostaglandins inhibit stomach fluid secretion and promote the secretion of cytoprotective mucus [14]. In addition, aspirin inhibits platelet aggregation, which leads to an increased risk of bleeding [15]. Enteric tablets and sustained-release formulations can reduce the mucosal damage caused by aspirin. However, mucosal damage cannot be completely avoided [16,17]. Gastrointestinal adverse effects were the leading cause of termination of aspirin treatment in patients [18].

Transdermal drug delivery is an effective method for reducing gastrointestinal adverse effects [19]. Transdermal drug delivery avoids the metabolism of aspirin in the gastrointestinal tract, which prevents direct contact between aspirin and COX-1 expressed in the gastric mucosa [20,21]. The transdermal delivery of aspirin may be a safer way to administer aspirin regularly [22]. The minimum effective dose of aspirin for antiplatelet aggregation is 75 mg/d [23,24]. Conventional patches or creams have difficulty achieving an effective dose of aspirin because of the barrier protective effects of the cuticle [25]. The aspirin loading and transdermal delivery efficiency must be sufficiently high to achieve an effective aspirin dose. The MN patch is a new dosage form that physically promotes transdermal drug delivery [26,27]. The MN tips can puncture the cuticle of the skin and deliver a drug to the epidermal and dermal layers [28,29]. MNs weaken the barrier protective effects of the cuticle and significantly increase the bioavailability of the drug compared to conventional patches [30,31]. MNs can be divided into several categories: solid, hollow, coated, and polymeric MNs [32]. Among them, polymeric MNs have been widely investigated for their brilliant biocompatibility, prominent biodegradability, and sufficient drug loading capacity [33,34].

We developed a dissolvable polymeric MN patch that allowed stable loading of aspirin in MNs for transdermal delivery. Aspirin is an unstable ester that is prone to spontaneous hydrolysis. Mixed solvents were used to dissolve the substrate materials and aspirin, which improved the stability of aspirin in the solution. The drying process was optimized to enhance the stability of aspirin in the MNs. A minimal amount of substrate material was added to provide the mechanical strength to the MNs, which allowed the MNs

to load with high levels of aspirin. The stability, mechanical strength, and puncture depth of aspirin-loaded MNs were evaluated *in vitro*. Pharmacokinetics and pharmacodynamics were evaluated in Sprague Dawley (SD) rats. The dissolution time of the MN tips and the skin recovery time were evaluated in Institute of Cancer Research (ICR) mice. Skin irritation in white Japanese rabbits was evaluated. This translational study provided a comprehensive study of aspirin-loaded MNs from an MN patch design to animal studies.

2. Materials and methods

2.1. Materials and animals

Aspirin was purchased from Solarbio (Beijing, China). Fluorescent red (FR), acetonitrile, adenosine diphosphate (ADP), phosphoric acid, and N,N-Dimethylacetamide (DMA) were purchased from SIGMA-ALDRICH (Missouri, USA). N-methylpyrrolidone (NMP) was purchased from Heowns Biochemical Technology Ltd (Tianjin, China). Dimethyl sulfoxide (DMSO) was purchased from Macklin Biochemical Co., Ltd (Shanghai, China). Isoflurane was purchased from Aladdin Biotechnology Co., Ltd (Shanghai, China). Hydroxypropyl methylcellulose (HPMC) was purchased from Shanhe Pharmaceutical Excipients Co. Ltd (Anhui, China). Polyvinyl alcohol (PVA) was purchased from Alpha Pharmaceutical Co. Ltd (Jiangxi, China). Polyvinylpyrrolidone (PVP) was purchased from Xinkaiyuan Pharmaceutical Co., Ltd (Henan, China). High-substituted hydroxypropylcellulose (HHPC) was purchased from Mreda (Beijing, China). ICR mice were obtained from Charles River (Beijing, China). SD rats and Japanese White rabbits were obtained from the Animal Experimentation centre of the Technical Institute of Physics and Chemistry, Chinese Academy of Sciences (Beijing, China).

2.2. MNs fabrication process

15% PVA was added to 22.5% water and dissolved by heating at 90 °C for 4 h. 20% aspirin and 10% PVP were dissolved by 32.5% DMA. The aqueous solution and the DMA solution were mixed and stirred thoroughly. The bubbles in the solution were removed through centrifugation at 5000 rpm for 10 min. Then, 35 μ l the solution was added to a PDMS mold. A pressure of –100 kPa was applied to the mold and held for 10 min. The solution entered the pinhole of the mold under negative pressure. The entire process of molding the MN solution took place at 4 °C. The mold containing the solution was placed in a dry box (DHG-9123A, Jing Hong, Shanghai, China) at 60 °C for 7.5 h to dry the MNs completely. Each MN patch loaded with 6 mg aspirin.

2.3. Simultaneous quantification of aspirin and salicylic acid

High-performance liquid chromatography (HPLC, DGU-20A3R, Shimadzu, Osaka, Japan) was used to quantify aspirin and salicylic acid. A YMC-Triart C18 column (YMC, Kyoto, Japan) was used for the separation at 30 °C. The mobile phase was a mixture of acetonitrile/0.3% phosphoric acid aqueous solution

(35/65, v/v). Isocratic elution was performed at a flow rate of 1.0 ml/min. Aspirin and salicylic acid were detected at 195 nm and 204 nm, respectively. The injection volume was 20 μ l and the time required for the analysis of each sample was 20 min.

2.4. Mechanical strength

A force-displacement test machine (AL-5 K, SA Precision Instruments, Shanghai, China) was used to test the mechanical strength of the MNs. MNs were fixed to the test platform by cyanoacrylate glue. The sensor probe (2×2 mm²) extruded 16 MNs along the axial direction at a speed of 1.1 mm/s. The force versus displacement curves of the MNs were recorded continuously in the range of 0–15 mN/needle.

2.5. Depth of puncture

A confocal laser scanning microscope (A1RMP, Nikon, Tokyo, Japan) was used to obtain images of the MNs puncturing the skin. The excitation and emission wavelengths of the FR were 510 nm and 600 nm, respectively. A laser with a wavelength of 530 nm was used to excite FR. The skin of an isolated porcine ear was used as a model skin [35]. The skin was scanned at a frequency of 20 μ m per time. The 3D reconstructed images were obtained using XYZ stacking.

2.6. In vivo pharmacokinetics

Male SD rats (256 ± 23 g) were randomly allocated to each group. A suspension containing 1 g/l aspirin was used for the gavage. The volume of the gavage was 2.5 ml/rat. Abdominal hair was removed using depilatory cream. At a predetermined time, blood was obtained from the tail vein and placed in a 1.5 ml heparin tube. The blood samples were centrifuged at 5,000 rpm for 10 min. The plasma supernatant was stored at -80 °C until analysis. 100 μ l plasma was injected into a 1.5 ml plastic centrifuge tube and extracted with 500 μ l acetonitrile by vortex mixing at 1,000 rpm for 40 min. The mixture was centrifuged at 12,000 rpm for 10 min at 4 °C, and the supernatant was collected for HPLC analysis.

2.7. In vivo pharmacodynamics

Male SD rats (247 ± 26 g) were randomly allocated to each group. After 7 d of continuous administration, blood samples were obtained from the tail vein. Plasma was separated from blood samples by centrifugation at 5000 rpm for 10 min. The plasma was stored frozen at -80 °C. Simultaneous quantification of thromboxane B₂ (TXB₂) in plasma was quantified using a TXB₂ ELISA kit (Cayman, USA). Platelet aggregation within 5 min was recorded using a 2-channel platelet aggregometer (700–2, Chrono-Log, USA). Aggregation was induced by ADP.

2.8. In vivo dissolution performance

MN patches were applied to male ICR mice. Abdominal hair was removed using depilatory cream. MN patches were applied to the abdominal skin of the mice with a force of 5 N/cm² and maintained for 30 s. The MN patches were

removed from the skin at preset time. The shape of the MNs was observed using an optical microscope (BX51, Olympus, Tokyo, Japan).

2.9. In vivo skin irritation

Skin irritation tests were performed on the dorsal skin of Japanese White rabbits [36]. Dorsal hair was removed using depilatory cream. MNs without aspirin and those loaded with aspirin were applied to the skin. The application time of MNs patch to the skin was 8 h. The skin surface was observed under an optical microscope.

3. Results and discussion

3.1. Hydrolysis of aspirin in solvents

Aspirin and salicylic acid were assayed simultaneously using HPLC. The retention time of aspirin and salicylic acid were 7.3 min and 10.8 min, respectively (Fig. 1A). The peak areas of both aspirin and salicylic acid were linearly correlated with solution concentration over the concentration range of 0.02–10 μ g/ml (Fig. 1B). Aspirin is slightly soluble in water (3.3 g/l, 20 °C). Water alone as a solvent did not allow the preparation of MNs with a high aspirin loading. The hydrolysis rate of aspirin was higher in water and lower in organic solvents. The ideal solvent for MNs should have a high solubility, low hydrolysis rate, and low boiling point. During the drying process of MNs, solvents with high boiling point required long heating time. A prolonged heating time results in a higher hydrolysis ratio of the aspirin-loaded in the MNs. Therefore, solvents with high boiling point are unsuitable for fabricating aspirin-loaded MNs. The stability of aspirin in the solution was enhanced by a mixture of water and organic solvents. The hydrolysis rate of aspirin in the solvent mixture was lower than the weighted mean of the hydrolysis rates in the single solvents (Fig. 1C–1E). The mixture of solvents also allows a wider range of polymeric materials to be dissolved, which provides a greater scope for screening substrate materials.

3.2. Hydrolysis of aspirin in solutions

Polymers were used as substrate materials to provide mechanical strength to the MNs [37]. The substrate materials accelerated the hydrolysis of aspirin in the solution. The type and concentration of the substrate material affected the hydrolysis rate of aspirin in the solution. The effects of the substrate materials on the hydrolysis of aspirin were discussed. The aspirin hydrolysis was irreversible. The ratio of aspirin hydrolysis in the solution gradually increased with time. The hydrolysis rate of aspirin in solution was accelerated with increasing concentrations of substrate materials in the range of 0–20%. PVP showed excellent compatibility with aspirin (Fig. 2A). HHP and HPMC had stronger promoting effects on aspirin hydrolysis (Fig. 2B–2C).

MNs containing only PVP and aspirin could not puncture the skin. PVA has great biocompatibility and little effect on aspirin hydrolysis [38]. PVA can be used as a water-soluble substrate material for aspirin-loaded MNs. The mixture of

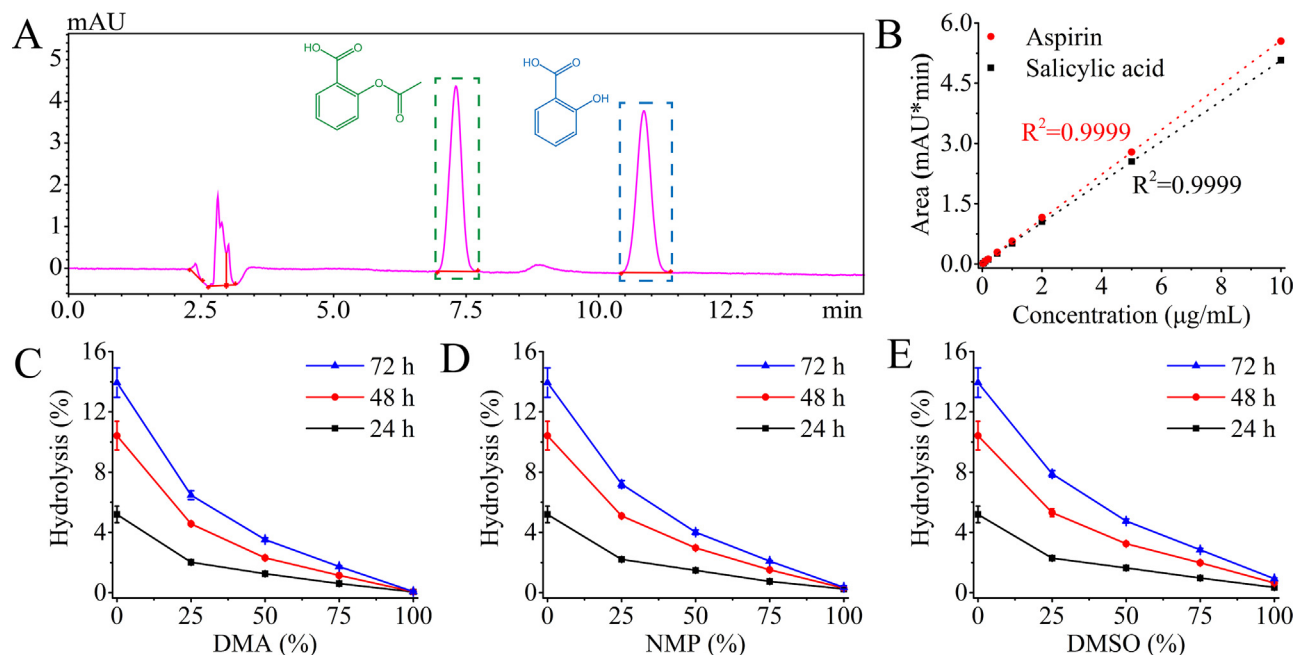


Fig. 1 - (A) The chromatogram of the mixture of aspirin and salicylic acid. **(B)** Calibration curves of aspirin and salicylic acid. **(C-E)** Hydrolysis ratios of aspirin in mixed solvents. The mixed solvent contained organic solvent and water. The organic solvents were DMA, NMP, and DMSO, respectively.

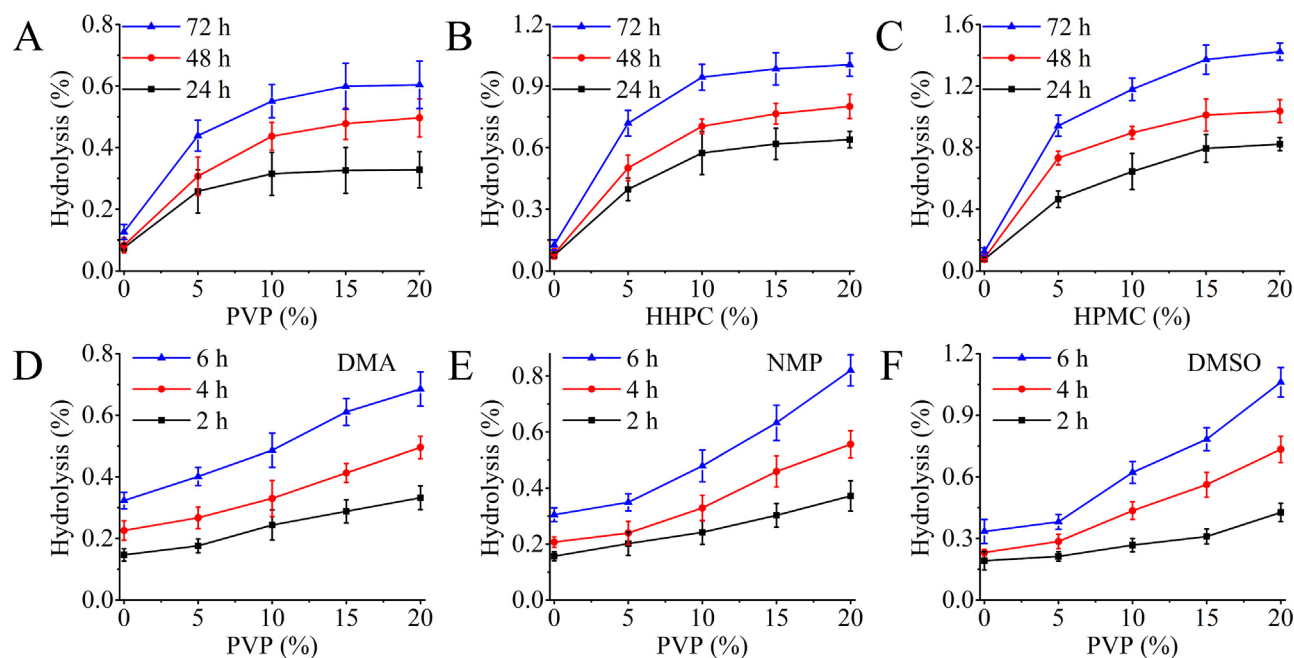


Fig. 2 - (A-C) Hydrolysis ratios of aspirin in solution. The solutions contained 20% aspirin, substrate material, and DMA. The substrate materials were PVP, HHPG, and HPMC, respectively. The substrate material and DMA accounted for a total of 80%. **(D-F)** Hydrolysis ratios of aspirin in solution. The solution contained 20% aspirin, 15% PVA, 22.5% water, PVP, and organic solvent. The organic solvents were DMA, NMP, and DMSO, respectively. The PVP and organic solvent accounted for a total of 42.5%.

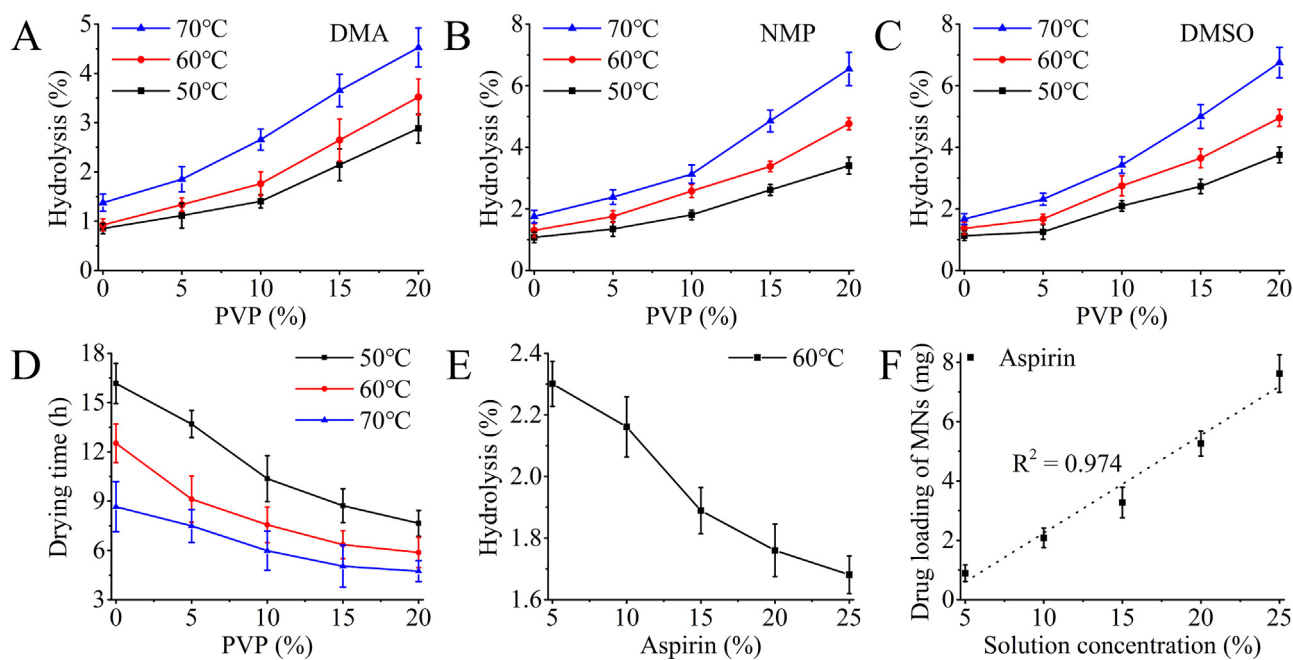


Fig. 3 – (A-C) Hydrolysis ratios of aspirin in MNs. The solution for the fabrication of MNs contained 20% aspirin, 15% PVA, 22.5% water, PVP, and organic solvent. The organic solvents were DMA, NMP, and DMSO, respectively. The PVP and organic solvent accounted for a total of 42.5%. (D) Drying time of MNs as a function of PVP content in solution. The solution for the fabrication of MNs contained 20% aspirin, 15% PVA, 22.5% water, PVP, and DMA. The PVP and DMA accounted for a total of 42.5%. (E) Hydrolysis ratios of aspirin in MNs as a function of the concentration of aspirin in solution. The solution contained 15% PVA, 10% PVP, 22.5% water, aspirin, and DMA. The aspirin and DMA accounted for a total of 52.5%. (F) The loading of aspirin in MNs as a function of the concentration of aspirin in the solution.

water and organic solvents can dissolve a wider variety of substrate materials. However, the hydrolysis rate of aspirin is higher in mixed solvents than in organic solvents. The ratio of water in the mixed solvent should be minimized as long as the substrate material is completely dissolved. An increase of PVP or PVA in the mixed solvent resulted in an increased hydrolysis rate of aspirin. The hydrolysis rate of aspirin was similar in the mixed solvents with DMA and NMP as organic solvents (Fig. 2D-2E). The hydrolysis rate of aspirin was relatively high in solvents mixed with DMSO as organic solvents (Fig. 2F). To reduce the hydrolysis rate of aspirin in MNs, the time for molding MNs should be under 2 h.

3.3. Hydrolysis of aspirin in MNs

The hydrolysis rate of aspirin in MNs is related to its prescription and drying conditions. The MNs were considered to be completely dry when the weight was constant. The hydrolysis rate of aspirin in the MNs increased with increasing drying temperature in the range of 50–70 °C (Fig. 3A-3C). The drying time of the MNs decreased with an increase of the drying temperature (Fig. 3D). The solution should contain not less than 15% PVA and 10% PVP. When the PVA content was less than 15%, the MNs did not have sufficient mechanical strength to puncture the skin. When the PVP content was less than 10%, the MNs curled during the drying process. The type and content of the substrate material in MNs should be minimized, which will reduce the hydrolysis rate of aspirin in the MNs.

The concentration of aspirin in the solution also affected its hydrolysis in the MNs. The rate of hydrolysis of aspirin in MNs decreased with increasing concentrations of aspirin in the range of 5%–25% (Fig. 3E). Increasing the concentration of aspirin in the solution decreased the drying time, leading to a decrease in the hydrolysis ratio of aspirin in MNs. In the range of 5%–25%, there was a linear correlation between the aspirin loading in the MNs and the concentration of aspirin in the solution (Fig. 3F). The aspirin loading in the MNs increased as the concentration of aspirin in the solution increased. The dose of MN administration was adjusted by changing the concentration of aspirin in the solution.

3.4. Mechanical strength of MNs

MNs must have sufficient mechanical strength to puncture the skin. MNs puncture the stratum corneum of the skin and create an array of micropores. Aspirin-loaded MNs should contain substrate material as few as possible under the premise that the skin can be punctured. The rate of hydrolysis of aspirin in MNs increased with the type and concentration of the substrate material. The MNs containing different levels of aspirin were tested for mechanical strength. The force-displacement curve had no inflection point, indicating that the MNs did not break under a force of 15 mN (Fig. 4A). In the range of 1–6 mg/patch, the mechanical strength of the MNs increased with increasing aspirin levels. The mechanical strength of MNs containing higher levels of aspirin decreased (Fig. 4D). The crystalline state of aspirin was observed in MNs

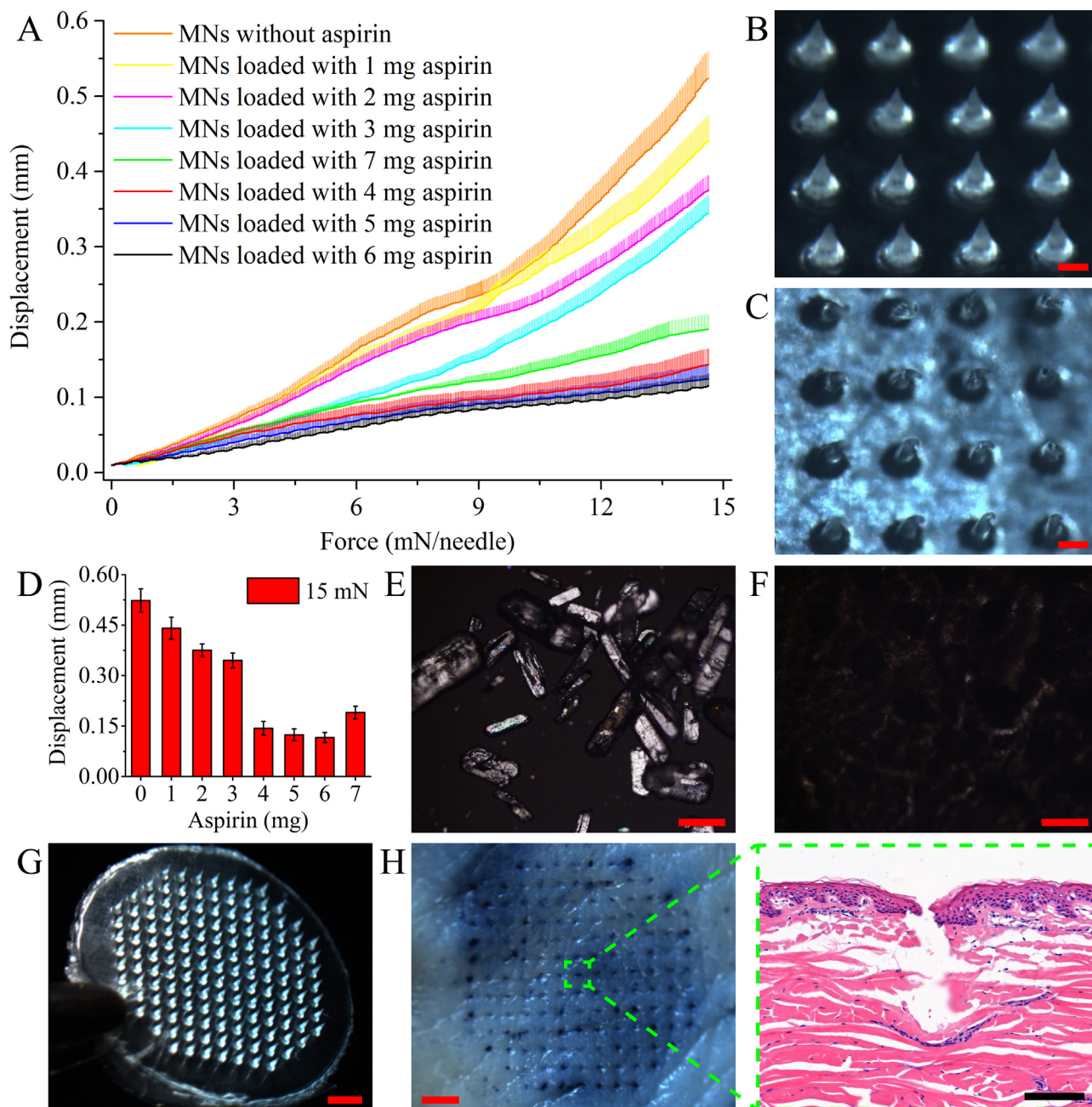


Fig. 4 – (A) Force-displacement curves of MNs loaded with different levels of aspirin. **(B)** Normal MNs (scale bar: 200 μ m). **(C)** MNs under 15 mN force along the axial direction (scale bar: 200 μ m). **(D)** Displacement of MNs under 15 mN force. **(E)** Polarizing microscope image of MNs loaded with 7 mg aspirin (scale bar: 100 μ m). **(F)** Polarizing microscope image of MNs loaded with 6 mg aspirin (scale bar: 100 μ m). **(G)** Optical microscope image of MN patch (scale bar: 1 mm). **(H)** Optical microscope image of an isolated porcine ear skin punctured by an MN patch loaded with 6 mg aspirin (scale bar: 1 mm). Inset: Optical microscope image of a paraffin section of the skin stained with H&E dye (scale bar: 100 μ m).

loaded with 7 mg aspirin (Fig. 4E). No crystals were observed in the MNs loaded with 1–6 mg aspirin (Fig. 4F). The crystalline state of aspirin weakens the mechanical strength of MNs.

All MNs were fabricated in the same PDMS mold. The mold was developed by Beijing CAS Microneedle Technology Ltd. The circular MN patch with a diameter of 1 cm included 145 MNs (Fig. 4G). The MN tip was a cone with a height of 500 μ m and a bottom diameter of 260 μ m. The spacing of

the MN tips was 500 μ m. After staining with trypan blue dye, the skin with MNs showed a clear array of micropores (Fig. 4H). Longitudinal sections of isolated porcine ear skin to which MNs were applied were stained with hematoxylin and eosin (H&E) dyes. Hematoxylin stained the nuclei blue, and eosin stained the cytoplasm pink [39]. The stratum corneum of the skin was punctured by the MNs, creating micropores that facilitated transdermal drug delivery. There

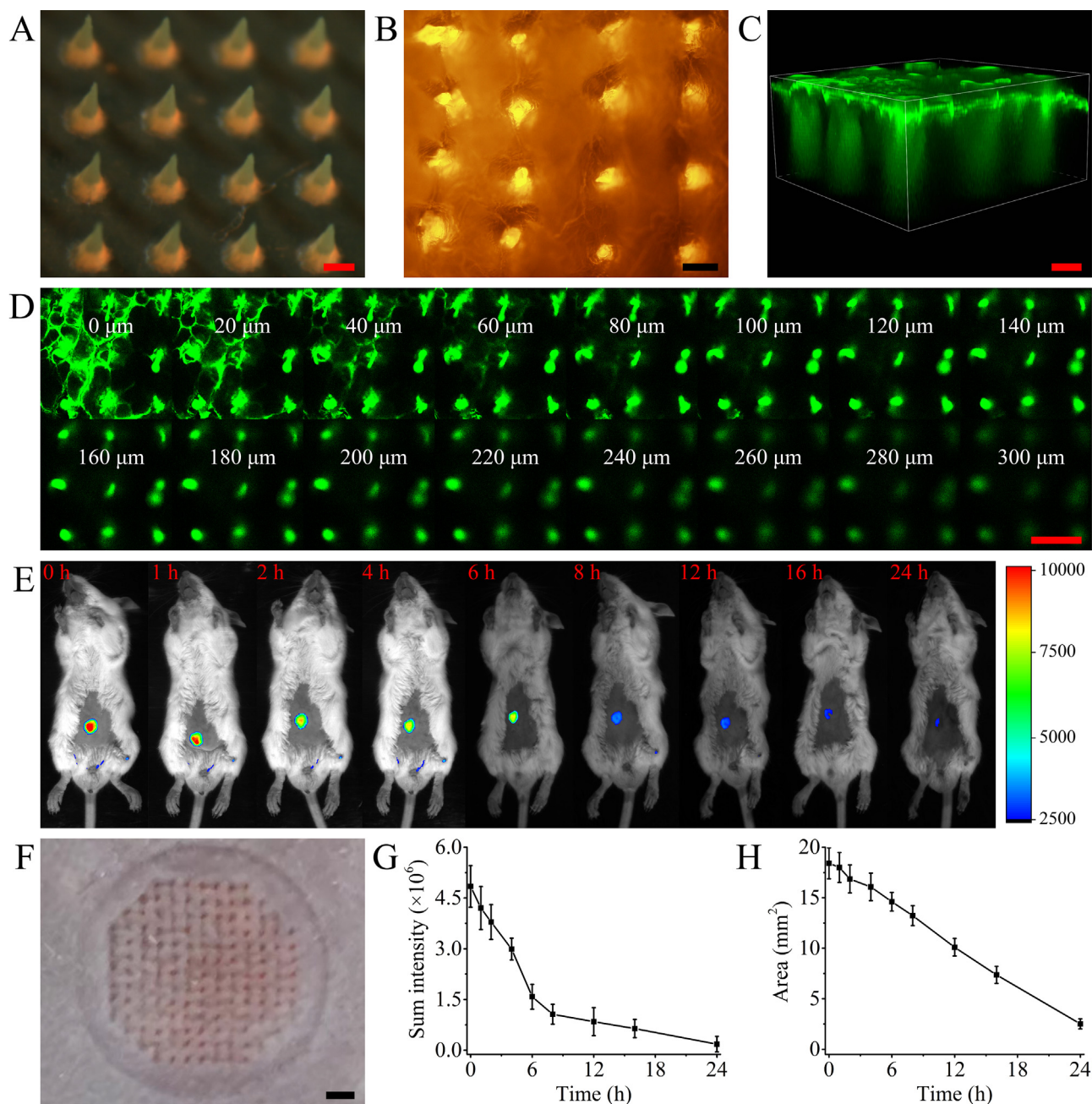


Fig. 5 – (A) Optical microscope image of MNs loaded with FR (scale bar: 200 μm). (B) Fluorescence microscope image of an isolated porcine ear skin punctured with MNs loaded with FR (scale bar: 200 μm). (C) 3D reconstruction image of the MN tips implantation site (scale bar: 100 μm). (D) Fluorescence imaging of the porcine ear skin at different depths (scale bar: 500 μm). (E) In vivo imaging of FR-loaded MNs implanted in the abdominal skin of ICR mice ($n = 6$). (F) Optical microscope image of the abdominal skin of an ICR mouse implanted with FR-loaded MNs (scale bar: 1 mm). (G) Curves of sum fluorescence intensity versus time. (H) Curves of fluorescent area versus time.

were no significant differences in microscope images of skin punctured by MN patches loaded with 1–6 mg aspirin.

3.5. Depth of MNs puncture of the skin

The depth at which the MNs puncture the skin determines the safety of the MNs [40]. To measure the puncture depth of the MNs, 2 mg/ml FR dye was added to the solution used to

fabricate the MNs loaded with FR (Fig. 5A). MNs loaded with FR were used to puncture isolated porcine ear skin (Fig. 5B). A confocal laser scanning microscope was used to observe the depth of the skin punctured by the MNs. Aspirin was delivered mainly through micropores in the skin. It was difficult to deliver aspirin through the stratum corneum in areas without micropores (Fig. 5C). The skin was punctured by the MNs to a depth of 300 μm (Fig. 5D).

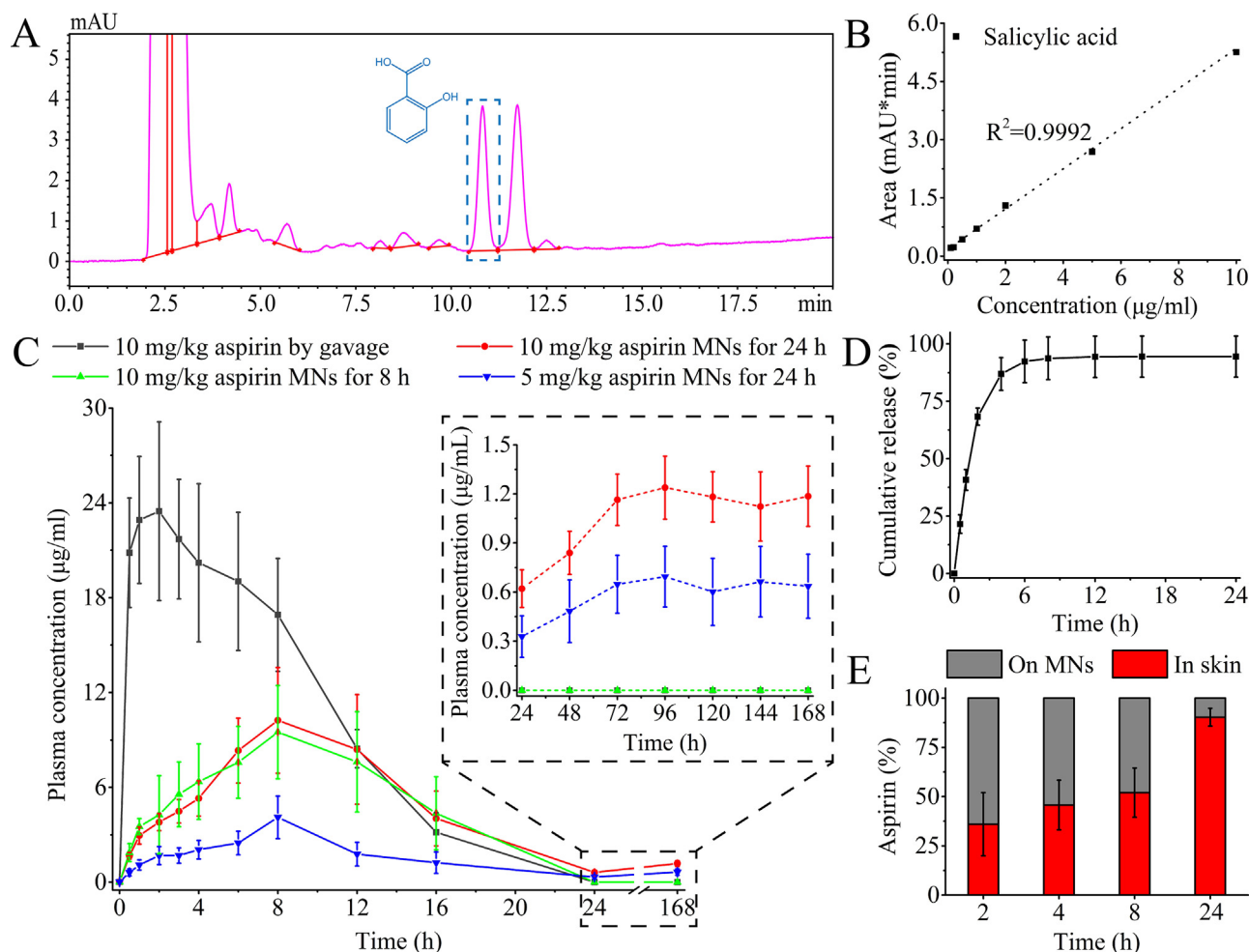


Fig. 6 – (A) The chromatogram of salicylic acid in SD rat plasma. **(B)** Calibration curves of salicylic acid in SD rat plasma. **(C)** Plasma concentrations of salicylic acid in SD rats after applying aspirin-loaded MNs ($n = 6$). **(D)** Cumulative release profile of aspirin-loaded MNs in phosphate buffer at pH 7.4. **(E)** The amount of aspirin residue in MNs after application to the skin of SD rats.

3.6. FR release from the MNs in vivo

FR was used as the model drug to evaluate the release rate of MNs loaded with insoluble drugs in mice. Whole-body imaging was carried out using an *in vivo* FX Pro imaging system (Eastman Kodak, NY, USA). The MNs loaded with FR dye were applied to the abdominal skin of ICR mice. The release of FR from MNs was visualized using *in vivo* imaging (Fig. 5E). The epidermis of mice applied with MNs appeared orange, indicating that the tips of the MNs had been implanted (Fig. 5F). Fluorescence intensity gradually decreased over time. Within 24 h, the fluorescence intensity decreased by 96.27% (Fig. 5G). The decrease in fluorescence intensity indicates the gradual diffusion of FR at the implantation site. The reduction in the fluorescence area lagged behind the fluorescence intensity, which indicated that the release of FR from the MNs was faster than the diffusion of FR in the skin (Fig. 5H).

3.7. Pharmacokinetic analysis of aspirin-loaded MNs

SD rats were used as model animals to evaluate the pharmacokinetic profile of the aspirin-loaded MNs. Aspirin

was hydrolyzed to salicylic acid in the plasma [41]. Salicylic acid in the plasma was detected using HPLC (Fig. 6A). The peak area was linearly correlated with the concentration of salicylic acid in plasma over the range of 0.1–10 µg/ml (Fig. 6B), $R^2=0.9992$). Phosphate buffer (pH 7.4) was used as the receiving solution to evaluate the rate of aspirin release from MNs. Aspirin in the MNs was released by 93.69% within 8 h (Fig. 6D). A positive correlation was observed between the quantity of aspirin entering the skin and the duration of attachment. The practical attachment time were 8 and 24 h, with 52.00% and 90.29% of aspirin entering the skin, respectively (Fig. 6E).

The time of peak plasma concentration (T_{max}) of oral aspirin in rats was 2 h. T_{max} for MN administration was 8 h (Fig. 6C). MN administration resulted in a smoother plasma concentration curve compared to oral administration. After MNs application, aspirin is released from the substrate materials and absorbed into the bloodstream by capillaries in the dermis [42]. There was no significant difference in plasma concentrations between rats with MNs attachment time of 8 and 24 h at the same dosage within 24 h. The rats were dosed on 7 successive d. Salicylic acid was not

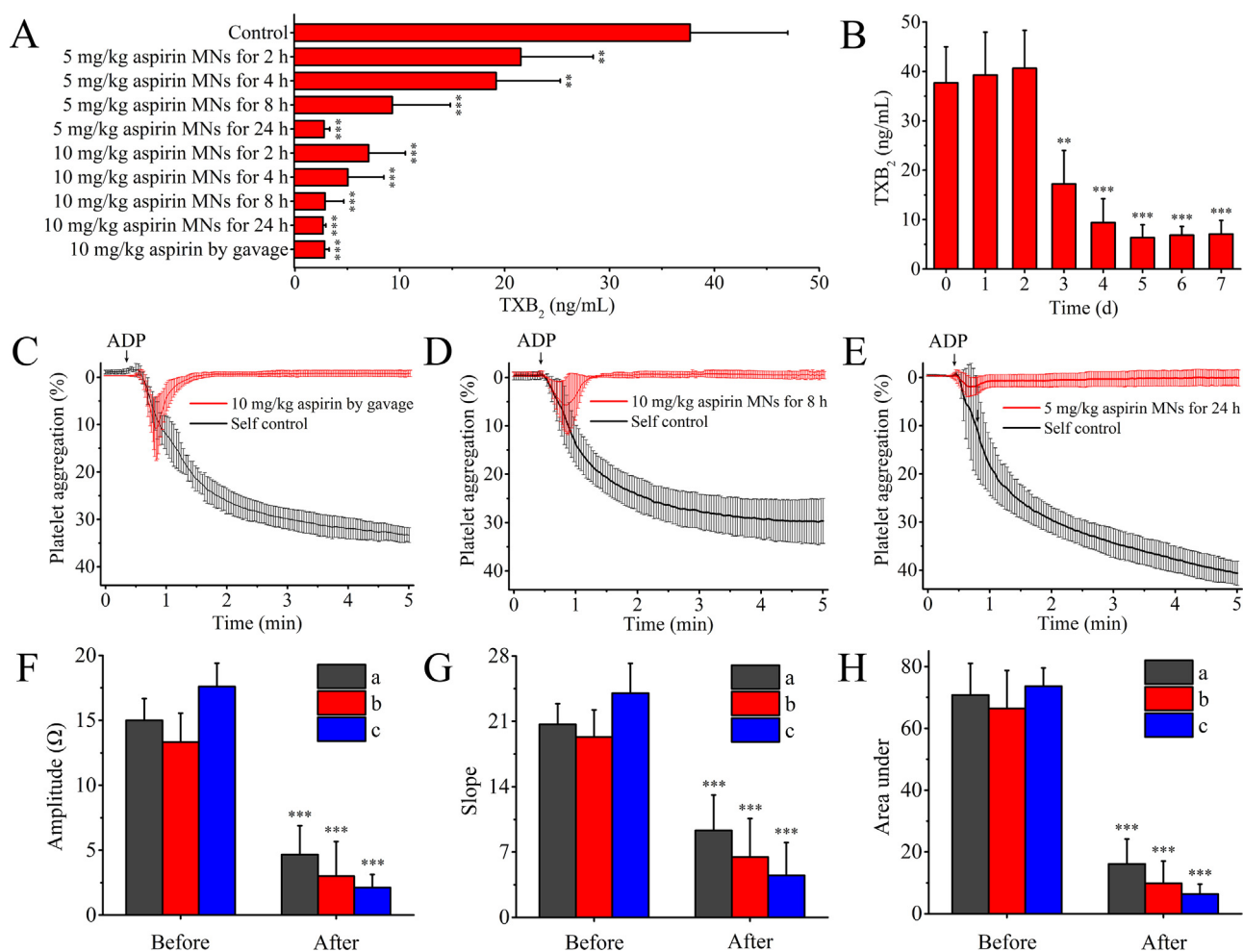


Fig. 7 – (A) Plasma concentration of TXB₂ in SD rats after 7 d of continuous administration (n = 6). (B) Plasma concentration of TXB₂ in SD rats versus time (n = 6). Rats were applied with 5 mg/kg of aspirin-loaded MNs for 24 h daily. (C-E) ADP induced platelet aggregation curves in rats (n = 6). (F-H) Characteristic parameters of platelet aggregation curves. a: 10 mg/kg aspirin by gavage. b: 10 mg/kg aspirin-loaded MNs for 8 h. c: 5 mg/kg aspirin-loaded MNs for 24 h. (F) Maximum amplitude of the platelet aggregation curve after ADP induction. (G) Mean slope of the platelet aggregation curve after ADP induction. (H) Area between platelet aggregation curve and X-axis after ADP induction. Compared with control group, *P < 0.05, **P < 0.01, *P < 0.001.**

detected in the plasma of rats with MNs attachment time of 8 h after each administration for 24 h. Salicylic acid in the plasma of rats did not accumulate during continuous dosing. Low concentrations of salicylic acid were detected in the plasma of rats with MNs attachment time of 24 h after each administration for 24 h. A small accumulation of salicylic acid concentrations in rat plasma during continuous dosing. After 3 d of continuous dosing, the accumulation of plasma concentrations stabilized. Aspirin in the backing layer of the MNs could be continuously delivered through the skin after the tips of the MN had dissolved.

3.8. Pharmacodynamic analysis of aspirin-loaded MNs

Antiplatelet aggregation by aspirin inhibits TXA₂ production. TXA₂ is a bioactive substance that is synthesized and released by platelet microsomes to promote vasoconstriction and platelet aggregation [43]. TXA₂ is rapidly metabolized to the

inactive TXB₂ in vivo [44]. The efficacy of aspirin could be evaluated by TXB₂ level in plasma. Oral administration of 10 mg/kg aspirin for seven consecutive d effectively inhibited TXB₂ levels in the plasma. MN patches of 5 mg/kg aspirin for 24 h or 10 mg/kg aspirin for 8 h achieved the same TXB₂ inhibitory effect as the oral administration of 10 mg/kg aspirin (Fig. 7A). The onset time of aspirin-loaded MNs inhibition of TXB₂ was evaluated. The plasma levels of TXB₂ in rats with continuous application of aspirin-loaded MNs for 3 d were significantly different from those in normal rats (Fig. 7B).

Platelet aggregation is the gold standard for measuring the efficacy of anticoagulants [45]. The efficacy of oral administration and MN administration for antiplatelet aggregation was evaluated. Continuous oral administration of 10 mg/kg aspirin for seven d significantly inhibited platelet aggregation in SD rats. MN patches of 5 mg/kg aspirin for 24 h or 10 mg/kg aspirin for 8 h achieved the same antiplatelet aggregation effect as oral administration of 10 mg/kg aspirin

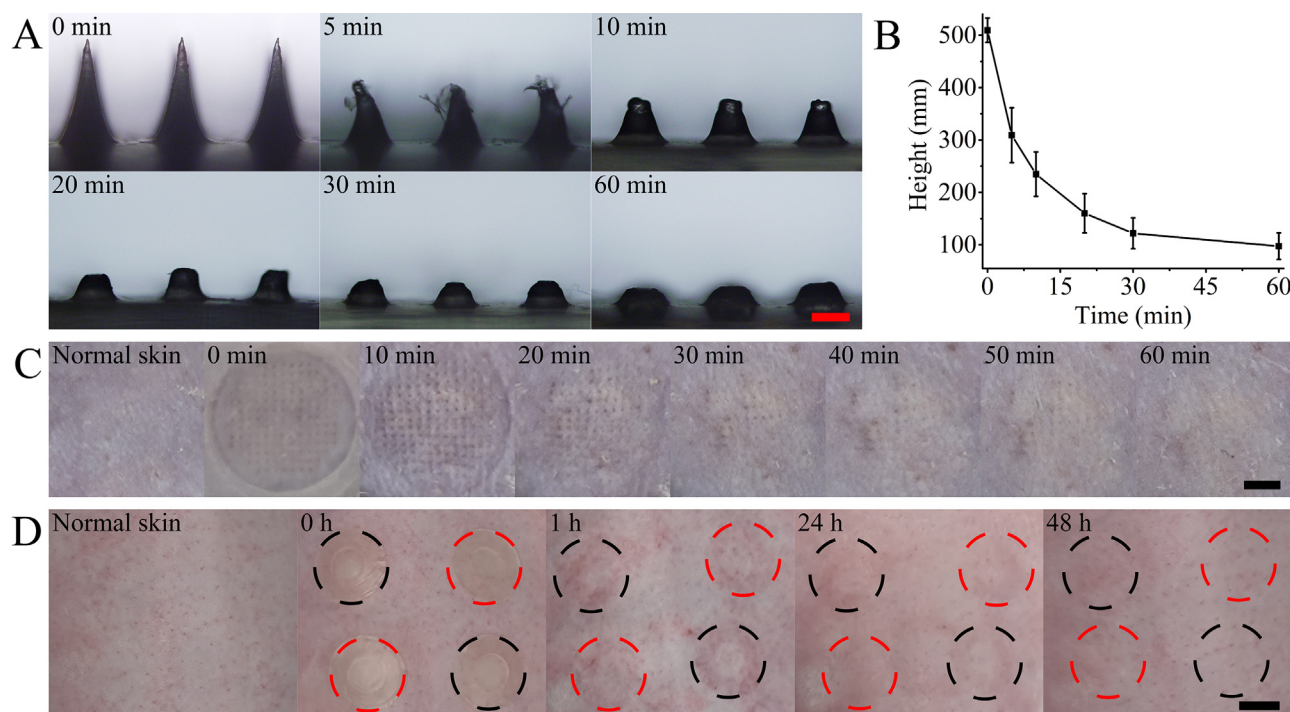


Fig. 8 – (A) Dissolution of MN tips in the abdominal skin of male ICR mice ($n = 6$, scale bar: 200 μm). (B) Variation of MN tips height with the time of MN patch application on the abdominal skin of male ICR mice. (C) Optical microscope image of the abdominal skin of ICR mice ($n = 3$, scale bar: 2 mm). (D) Optical microscope image of the dorsal skin of male Japanese White rabbits after MN patch application. The black dashed circles indicated the areas where MN patch without aspirin were applied. The red dashed circles indicated the areas where MN patch loaded with 6 mg aspirin per patch were applied ($n = 3$, scale bar: 10 mm).

(Fig. 7C-7E). The amplitude, slope, and area under the curve are characteristic parameters of the platelet aggregation curve. All three characteristic parameters were significantly different before and after drug administration (Fig. 7F-7H). The pharmacodynamic analysis demonstrated that MNs transdermal delivery of aspirin was an effective mode of administration.

3.9. Skin irritation of MNs

The dissolution rate of the MN tips in the skin is related to the substrate material [46]. Dissolution of the MN tips in the skin of ICR mice was observed under a microscope (Fig. 8A). The MN tips implanted into the skin gradually dissolved over time. The height of the MN tips was reduced by 80.89% within 60 min (Fig. 8B). The abdominal skin of the ICR mice was smooth and intact before MN patch application. An array of micropores appeared on the skin after the MN patch was applied and maintained for 10 min. The micropores on the skin gradually recovered over time after the removal of the MN patch. Under the microscope, the skin recovered completely within 60 min (Fig. 8C). Skin irritation was observed after the application of the MN patch in Japanese White rabbits. There was slight erythema on the skin at the site of the MN patch application. No edema or scabbing was observed. Erythema was a localized microinjury caused by MN tips puncturing the skin. The erythema on the skin completely recovered under the microscope within

24 h. There was no significant difference in the skin between the aspirin-loaded MN patch and MN patch without aspirin (Fig. 8D). This demonstrated that aspirin did not evoke primary irritation in MN patch. And it improved the rate of transdermal delivery of aspirin while ensuring safety.

4. Conclusions

In this study, we developed a dissolvable polymeric MN patch loaded with aspirin. Factors affecting the stability of aspirin in MNs were comprehensively researched. To improve the stability of aspirin in MNs, as few as possible substrate material was added to ensure that the MNs had sufficient mechanical strength to puncture the skin. The hydrolysis rate of aspirin in the MNs was less than 2%. MN administration of aspirin resulted in a smoother plasma concentrations curve compared to oral administration. Inhibition of TXA_2 production and antiplatelet aggregation by aspirin-loaded MNs were demonstrated in SD rats. MN administration of aspirin had a lower effective dose than oral administration. A skin irritation study was performed on the skin of the Japanese White rabbits. Only slight erythema was observed on the skin, which recovered within 24 h. Aspirin has been used for antiplatelet aggregation for over 120 years. Improving the efficacy and reducing gastrointestinal adverse effects remain the primary goals for developing novel dosage forms of aspirin [47]. MN administration of aspirin offers a novel option for

patients taking aspirin regularly and it is a new method to reduce the gastrointestinal adverse effects of non-selective cyclooxygenase inhibitors.

Conflicts of interest

The authors report no conflicts of interest.

Acknowledgement

This work was supported by the National Key Research and Development Plan of China [No. 2016YFC1000902].

REFERENCES

- [1] Mehta SR, Yusuf S, Peters RJG, Bertrand ME, Lewis BS, Natarajan MK, et al. Effects of pretreatment with clopidogrel and aspirin followed by long-term therapy in patients undergoing percutaneous coronary intervention: the PCI-CURE study. *Lancet* 2001;358:527–33.
- [2] Angiolillo DJ, Rollini F, Storey RF, Bhatt DL, James S, Schneider DJ, et al. International expert consensus on switching platelet P2Y₁₂ receptor-inhibiting therapies. *Circulation* 2017;136(20):1955–75.
- [3] Bos CL, Richel DJ, Ritsema T, Peppelenbosch MP, Versteeg HH. Prostanoids and prostanoid receptors in signal transduction. *Int J Biochem Cell Biol* 2004;36(7):1187–205.
- [4] Fuentes E, Palomo I. Mechanism of antiplatelet action of hypolipidemic, antidiabetic and antihypertensive drugs by PPAR activation: PPAR agonists: new antiplatelet agents. *Vascul Pharmacol* 2014;62(3):162–6.
- [5] Bhatt DL, Grosser T, Dong JF, Logan D, Jeske W, Angiolillo DJ, et al. Enteric coating and aspirin nonresponsiveness in patients with type 2 diabetes mellitus. *J Am Coll Cardiol* 2017;69(6):603–12.
- [6] Ammar HO, Ghorab M, El-Nahas SA, Kamel R. Design of a transdermal delivery system for aspirin as an antithrombotic drug. *Int J Pharm* 2006;327(1–2):81–8.
- [7] Rowland M, Riegelman S, Harris PA, Sholkoff SD. Absorption kinetics of aspirin in man following oral administration of an aqueous solution. *J Pharm Sci* 1972;61:379–85.
- [8] Lucotti S, Cerutti C, Soyer M, Gil-Bernabe AM, Gomes AL, Allen PD, et al. Aspirin blocks formation of metastatic intravascular niches by inhibiting platelet-derived COX-1/thromboxane A₂. *J Clin Invest* 2019;129(5):1845–62.
- [9] Crescente M, Menke L, Chan MV, Armstrong PC, Warner TD. Eicosanoids in platelets and the effect of their modulation by aspirin in the cardiovascular system (and beyond). *Br J Pharmacol* 2019;176(8):988–99.
- [10] Quach ME, Chen WC, Li RH. Mechanisms of platelet clearance and translation to improve platelet storage. *Blood* 2018;131:1512–21.
- [11] Wallace JL. Prostaglandins, NSAIDs, and gastric mucosal protection: why doesn't the stomach digest itself? *Physiol Rev* 2008;88(4):1547–65.
- [12] Xu XR, Yousef GM, Ni H. Cancer and platelet crosstalk: opportunities and challenges for aspirin and other antiplatelet agents. *Blood* 2018;131:1777–89.
- [13] Ridker PM, Cook NR, Lee NR, Gordon D, Gaziano JM, Manson JE, et al. A randomized trial of low-dose aspirin in the primary prevention of cardiovascular disease in women. *N Engl J Med* 2005;352:1293–304.
- [14] Laine L, Takeuchi K, Tarnawski A. Gastric mucosal defense and cytoprotection: bench to bedside. *Gastroenterology* 2008;135(1):41–60.
- [15] Rayes HA, Subat YW, Weister T, Johnson MQ, Hanson A, Schulte PJ, et al. Concomitant aspirin and anticoagulation is associated with increased risk for major bleeding in surgical patients requiring postoperative intensive care. *Crit Care Med* 2020;48(7):985–92.
- [16] Watanabe T, Sugimori S, Kameda N, Machida H, Okazaki H, Tanigawa T, et al. Small bowel injury by low-dose enteric-coated aspirin and treatment with misoprostol: a pilot study. *Clin Gastroenterol Hepatol* 2008;6(11):1279–82.
- [17] Khaled SA, Burley JC, Alexander MR, Yang J, Roberts CJ. 3D printing of five-in-one dose combination polypill with defined immediate and sustained release profiles. *J Control Release* 2015;217:308–14.
- [18] Pirmohamed M, James S, Meakin S, Green C, Scott AK, Walley TJ, et al. Adverse drug reactions as cause of admission to hospital: prospective analysis of 18820 patients. *Br Med J* 2004;329:15–19.
- [19] Kumar R, Chen M, Parmar VS, Samuelson LA, Kumar J, Nicolosi R, et al. Supramolecular assemblies based on copolymers of PEG600 and functionalized aromatic diesters for drug delivery applications. *J Am Chem Soc* 2004;126:10640–4.
- [20] Zuo J, Du L, Li M, Liu B, Zhu W, Jin Y. Transdermal enhancement effect and mechanism of iontophoresis for non-steroidal anti-inflammatory drugs. *Int J Pharm* 2014;466(1–2):76–82.
- [21] Yi QF, Yan J, Tang SY, Huang H, Kang LY. Effect of borneol on the transdermal permeation of drugs with differing lipophilicity and molecular organization of stratum corneum lipids. *Drug Dev Ind Pharm* 2016;42(7):1086–93.
- [22] He X, Sun J, Zhuang J, Xu H, Liu Y, Wu D. Microneedle system for transdermal drug and vaccine delivery: devices, safety, and prospects. *Dose Response* 2019;17(4):1–18.
- [23] Gilard M, Arnaud B, Cornily JC, Le Gal G, Lacut K, Le Calvez G, et al. Influence of omeprazole on the antiplatelet action of clopidogrel associated with aspirin: the randomized, double-blind OCLA (Omeprazole CLopidogrel Aspirin) study. *J Am Coll Cardiol* 2008;51(3):256–60.
- [24] Cuzick J, Thorat MA, Bosetti C, Brown PH, Burn J, Cook NR, et al. Estimates of benefits and harms of prophylactic use of aspirin in the general population. *Ann Oncol* 2015;26(1):47–57.
- [25] Olatunji O, Olubowale M, Okereke C. Microneedle-assisted transdermal delivery of acetylsalicylic acid (aspirin) from biopolymer films extracted from fish scales. *Polym Bull* 2018;75(9):4103–15.
- [26] Cao S, Wang Y, Wang M, Yang X, Tang Y, Pang M, et al. Microneedles mediated bioinspired lipid nanocarriers for targeted treatment of alopecia. *J Control Release* 2021;329:1–15.
- [27] Chen SX, Ma M, Xue F, Shen S, Chen Q, Kuang Y, et al. Construction of microneedle-assisted co-delivery platform and its combining photodynamic/immunotherapy. *J Control Release* 2020;324:218–27.
- [28] Arora A, Prausnitz MR, Mitragotri S. Micro-scale devices for transdermal drug delivery. *Int J Pharm* 2008;364(2):227–36.
- [29] Chen Y, Yang Y, Xian Y, Singh P, Feng J, Cui S, et al. Multifunctional graphene-oxide-reinforced dissolvable polymeric microneedles for transdermal drug delivery. *ACS Appl Mater Interfaces* 2020;12(1):352–60.
- [30] Volpe-Zanutto F, Ferreira LT, Permana AD, Kirkby M, Paredes AJ, Vora LK, et al. Artemether and lumefantrine dissolving microneedle patches with improved pharmacokinetic performance and antimalarial efficacy in mice infected with *Plasmodium yoelii*. *J Control Release* 2021;333:298–315.

- [31] Yang L, Liu Q, Wang X, Gao N, Li X, Chen H, et al. Actively separated microneedle patch for sustained-release of growth hormone to treat growth hormone deficiency. *Acta Pharm Sin B* 2022;17:70–86.
- [32] Ita K. Transdermal delivery of drugs with microneedles: strategies and outcomes. *J Drug Deliv Sci Tec* 2015;29:16–23.
- [33] Yang L, Yang Y, Chen H, Mei L, Zeng X. Polymeric microneedle-mediated sustained release systems: design strategies and promising applications for drug delivery. *Asian J Pharm Sci* 2021;17(1):70–86.
- [34] Wu M, Xia T, Li Y, Wang T, Yang S, Yu J, et al. Design and fabrication of r-hirudin loaded dissolving microneedle patch for minimally invasive and long-term treatment of thromboembolic disease. *Asian J Pharm Sci* 2022;17(2):284–97.
- [35] Vitorino C, Almeida A, Sousa J, Lamarche I, Gobin P, Marchand S, et al. Passive and active strategies for transdermal delivery using co-encapsulating nanostructured lipid carriers: in vitro vs. in vivo studies. *Eur J Pharm Biopharm* 2014;86(2):133–44.
- [36] Xing M, Yang G, Zhang S, Gao Y. Acid-base combination principles for preparation of anti-acne dissolving microneedles loaded with azelaic acid and matrine. *Eur J Pharm Sci* 2021;165:105935–46.
- [37] Ye Y, Yu J, Wen D, Kahkoska AR, Gu Z. Polymeric microneedles for transdermal protein delivery. *Adv Drug Deliv Rev* 2018;127:106–18.
- [38] Ding Q, Xu X, Yue Y, Mei C, Huang C, Jiang S, et al. Nanocellulose-mediated electroconductive self-healing hydrogels with high strength, plasticity, viscoelasticity, stretchability, and biocompatibility toward multifunctional applications. *ACS Appl Mater Interfaces* 2018;10(33):27987–8002.
- [39] Li G, Badkar A, Nema S, Kolli CS, Banga AK. In vitro transdermal delivery of therapeutic antibodies using maltose microneedles. *Int J Pharm* 2009;368(1–2):109–15.
- [40] Yu W, Jiang G, Zhang Y, Liu D, Xu B, Zhou J. Polymer microneedles fabricated from alginate and hyaluronate for transdermal delivery of insulin. *Mater Sci Eng C Mater Biol Appl* 2017;80:187–96.
- [41] Tang M, Mukundan M, Yang J, Charpentier N, LeCluyse EL, Black C, et al. Antiplatelet agents aspirin and clopidogrel are hydrolyzed by distinct carboxylesterases, and clopidogrel is transesterificated in the presence of ethyl alcohol. *J Pharmacol Exp Ther* 2006;319(3):1467–76.
- [42] Samant PP, MR P. Mechanisms of sampling interstitial fluid from skin using a microneedle patch. *P Natl Acad Sci USA* 2018;115(18):4583–8.
- [43] Cheng Y, Austin SC, Rocca B, Koller BH, Coffman TM, Grosser T, et al. Role of prostacyclin in the cardiovascular response to thromboxane A₂. *Science* 2002;296:539–41.
- [44] Patrono C, Rocca B. Measurement of thromboxane biosynthesis in health and disease. *Front Pharmacol* 2019;10:1244–55.
- [45] Gaziano JM, Brotons C, Coppolecchia R, Cricelli C, Darius H, Gorelick PB, et al. Use of aspirin to reduce risk of initial vascular events in patients at moderate risk of cardiovascular disease (ARRIVE): a randomised, double-blind, placebo-controlled trial. *Lancet* 2018;392(10152):1036–46.
- [46] Yan L, Raphael AP, Zhu X, Wang B, Chen W, Tang T, et al. Nanocomposite-strengthened dissolving microneedles for improved transdermal delivery to human skin. *Adv Healthc Mater* 2014;3(4):555–64.
- [47] Xie F, Chai JK, Hu Q, Yu YH, Ma L, Liu LY, et al. Transdermal permeation of drugs with differing lipophilicity: effect of penetration enhancer camphor. *Int J Pharm* 2016;507(1–2):90–101.